HHS Public Access

Author manuscript

Radiat Res. Author manuscript; available in PMC 2023 May 12.

Published in final edited form as:

Radiat Res. 2022 August 01; 198(2): 181–189. doi:10.1667/RADE-21-00232.1.

Oxygen Monitoring in Model Solutions and *In Vivo* in Mice During Proton Irradiation at Conventional and FLASH Dose Rates

Alexander L. Van Slyke[a,1], **Mirna El Khatib**[b,1], **Anastasia Velalopoulou**[a], **Eric Diffenderfer**[a], **Khayrullo Shoniyozov**[a], **Michele M. Kim**[a], **Ilias V. Karagounis**[a], **Theresa M. Busch**[a], **Sergei A. Vinogradov**[b], **Cameron J. Koch**[a], **Rodney D. Wiersma**[a,2]

[a]Department of Radiation Oncology, University of Pennsylvania, Philadelphia

[b]Department of Biochemistry and Biophysics, Perelman School of Medicine, and Department of Chemistry, School of Arts and Sciences, University of Pennsylvania, Philadelphia, Pennsylvania

Abstract

FLASH is a high-dose-rate form of radiation therapy that has the reported ability, compared with conventional dose rates, to spare normal tissues while being equipotent in tumor control, thereby increasing the therapeutic ratio. The mechanism underlying this normal tissue sparing effect is currently unknown, however one possibility is radiochemical oxygen depletion (ROD) during dose delivery in tissue at FLASH dose rates. In order to investigate this possibility, we used the phosphorescence quenching method to measure oxygen partial pressure before, during and after proton radiation delivery in model solutions and in normal muscle and sarcoma tumors in mice, at both conventional (Conv) (~0.5 Gy/s) and FLASH (~100 Gy/s) dose rates. Radiation dosimetry was determined by Advanced Markus Chamber and EBT-XL film. For solutions contained in sealed glass vials, phosphorescent probe Oxyphor PtG4 (1 μM) was dissolved in a buffer (10 mM HEPES) containing glycerol (1 M), glucose (5 mM) and glutathione (5 mM), designed to mimic the reducing and free radical-scavenging nature of the intracellular environment. *In vivo* oxygen measurements were performed 24 h after injection of PtG4 into the interstitial space of either normal thigh muscle or subcutaneous sarcoma tumors in mice. The “g-value” for ROD is reported in mmHg/Gy, which represents a slight modification of the more standard chemical definition (μM/Gy). In solutions, proton irradiation at conventional dose rates resulted in a g-value for ROD of up to 0.55 mmHg/Gy, consistent with earlier studies using X or gamma rays. At FLASH dose rates, the g-value for ROD was ~25% lower, 0.37 mmHg/Gy. pO_2 levels were stable after each dose delivery. For normal muscle *in vivo*, oxygen depletion during irradiation was counterbalanced by resupply from the vasculature. This process was fast enough to maintain tissue pO_2 virtually unchanged at Conv dose rates. However, during FLASH irradiation there was a stepwise decrease in pO_2 (g-value ~0.28 mmHg/Gy), followed by a rebound to the initial level after ~8 s. The g-values were smaller and recovery times longer in tumor tissue when compared to muscle and may be related to the lower initial endogenous pO_2 levels in the former. Considering that the FLASH effect is seen *in vivo* even at doses as low as 10 Gy, it is difficult to

[2]Corresponding author: Department of Biochemistry and Biophysics, Perelman School of Medicine, and Department of Chemistry, School of Arts and Sciences, University of Pennsylvania, Philadelphia, PA; rodney.wiersma@pennmedicine.upenn.edu.
[1]Shared co-first authorship.

reconcile the amount of protection seen by oxygen depletion alone. However, the phosphorescence probe in our experiments was confined to the extracellular space, and it remains possible that intracellular oxygen depletion was greater than observed herein. In cell-mimicking solutions the oxygen depletion g-vales were indeed significantly higher than observed *in vivo*.

INTRODUCTION

Delivery of radiation for the purpose of tumor control while minimizing negative effects on surrounding normal tissues is of primary concern in radiation oncology. Recent studies have demonstrated that ultra-high dose rate (>40 Gy/s) radiotherapy (RT), known as FLASH-RT, provides a normal-tissue sparing effect while maintaining tumor control, thereby increasing the therapeutic ratio (1, 2). This protective effect in normal tissue was first demonstrated in murine models using electron RT (3). Consequently, the FLASH effect has been demonstrated in various tissue types and across multiple species (4–6). More recently, the effect has been investigated using proton radiotherapy, with mixed results (7, 8).

Of several mechanisms critical to modification of radiation response, the “oxygen effect” acts to decrease radiation-induced damage as the oxygen concentration decreases (9–11). At the same time, oxygen is depleted by radiation via oxidation of multiple organic radicals that are produced (12, 13). Hence, a possible mechanism to explain radioprotection by FLASH in normal tissue is the increase in radiation resistance accompanying radiochemical oxygen depletion (ROD) during the dose administration (14–17).

Over many decades, chemical and biochemical oxygen consumption under a wide range of conditions has typically been measured using Clark polarographic oxygen sensors (18). These sensors have widely varying sensitivity and accuracy, and their response times are extensive due to the slow diffusion of oxygen through the membrane used to separate the active electrode surface from the measurement medium (19). They have been adapted as needle sensors for use *in vivo*, but are invasive and unable to make more than approximately 1 measurement per second. Additionally needle sensors cannot be used to make multiple measurements in the same position as a function of time (20). Polarographic oxygen sensors have been used for measurements of ROD in a few papers (12, 13), but due to their slow response times they cannot track the rapid oxygen changes during FLASH irradiation.

An alternative oxygen measurement technique, based on the oxygen-dependent quenching of phosphorescence, was introduced by Wilson and co-workers in 1987 (21). This technique requires the administration of a molecular phosphorescent probe. Probes have been developed that allow measurements of oxygen partial pressures in tissues *in vivo* and could be suitable for oxygen monitoring during FLASH (22–25).

The first use of the phosphorescence quenching method to monitor the effects of electron exposure on tissue oxygenation was recently published (25). However, the reported measurement rates were restricted (due to instrumentation limitations) to approximately 7/s, and could not be used during FLASH irradiation due to Cherenkov radiation and other light emission associated with the high-energy-electron radiation source. These limitations demonstrated the need for a much faster measurement technique, coupled with a radiation

source (e.g., non-relativistic protons) likely to cause much reduced light emission in the samples and optical fibers (26). Such a technique has been recently developed wherein it was confirmed that protons comprise a suitable radiation source (27).

In this work, we used the new technique to perform measurements with the goal to quantify the effect of dose rate, initial oxygen partial pressure, total dose delivered, and the presence of free radical scavengers on the g-value for oxygen partial pressure depletion (quantified herein in mmHg/Gy), both for conventional and FLASH-proton irradiation (0.5 Gy/s and 100 Gy/s, respectively). In particular, for *ex vivo* model measurements we used a solution designed to mimic key properties of the intracellular milieu with respect to ROD, consisting of HEPES (10 mM), glycerol (1 M), glucose (5 mM) and glutathione (5 mM). Also, in this study, we monitored oxygen levels *in vivo* in normal muscle and sarcoma tumors of mice during proton FLASH treatment with high temporal resolution.

METHODS

Proton Irradiation Setup

This study utilized the setup previously described by Diffenderfer *et al.* (8) with modifications to accommodate optical fibers and glass vials (27). In particular, an IBA Proteus Plus system (Louvain-La-Neuve, Belgium) delivered protons at 230 MeV to a dedicated research room via a collimated double scattering system (Fig. 1). At this energy, one would expect no Cherenkov emission from the protons, only that from rare fast electrons or scintillation from other materials within the beam (26). Dose rate and beam profile at the isocenter was measured prior to each experiment using a parallel plate Advanced Markus Chamber (PTW, Freiburg, Germany) and EBT-XL film (Ashland Advanced Materials, Bridgewater, NJ), respectively. The protons were delivered in 2 ns pulses at 106 MHz, corresponding to the cyclotron radio frequency. This pulse structure is particularly suitable for our measurement technique because it can be considered a constant source of radiation over the ~0.3 ms period of each measurement.

For experiments using model solutions of chemicals, a circular collimator (2.6-cm diameter) was used, and an acrylic block was fabricated with a cylindrical hole that positioned the center of the screw-cap glass sample vial (Fisher 03-339-21B) at beam isocenter to ensure complete irradiation of the vial contents. The acrylic block had two additional holes perpendicular to the beam path to position the optical fibers needed for oxygen partial pressure monitoring (Fig. 1A).

For *in vivo* experiments, a 2-cm square collimator was used to irradiate the leg, and the anesthetized mice were secured with tape to a heating pad in a position that minimized abdominal radiation exposure (Fig. 1B).

Oxygen Measurements by Phosphorescence Quenching

Oxygen partial pressure (pO_2) measurements, both in model solutions and *in vivo*, were performed using an Oxyled phosphorometer (Oxygen Enterprises) and the phosphorescent probe Oxyphor PtG4 (24). As described in detail in our recent study (27), the instrument was modified from its standard operation, which involved calculating an oxygen partial pressure

after averaging the analysis of many decays at an overall frequency of approximately 7 measurements per second. For high-speed acquisition, the phosphorometer sent a raw data stream of consecutive phosphorescence excitations and decays to the computer for subsequent analysis. The phosphorescence lifetime of Oxyphor PtG4 in an aqueous environment in the absence of oxygen is 51 μs at 23°C and 49.5 μs at 37°C. Since the probe was chemically inert, calibrations were only required for testing of new batches of the probe. The instrument reports oxygen partial pressure in mmHg so g-values for oxygen depletion were reported as mmHg/Gy rather than the standard chemical definition of μM/Gy. This was done for consistency since absolute oxygen concentrations *in vivo* can only be estimated and vary with the local environment. Phosphorescence decay measurements were performed with repetition rates of up to 3 kHz. Despite lack of Cherenkov from the incident protons, additional light pulses were observed, especially during the FLASH doses (27). These were removed by a software algorithm as described elsewhere (27) and some averaging was done to further reduce the noise. Thus, averaging in bins of 10 sequential decays gave an effective measurement rate of ~300 Hz. The Oxyled phosphorometer had two selectable light sources; a light emitting diode, whose output was coupled via an optical cable, and a laser diode whose output was directly transmitted by air to the desired location, with focusing provided by an integral lens. The approximate beam-diameters on the surface of the object for these two light sources were 5 mm and 0.2 mm, respectively.

Radiochemical Oxygen Depletion in Model Solutions

ROD in completely filled glass vials was quantified by measuring phosphorescence of Oxyphor PtG4 (1 μM final concentration) in aqueous solutions designed to partially mimic the intracellular milieu in terms of total free-radical scavenging ability and reducing nature (CELL) (28). CELL was composed of glycerol (1 M), glucose (5 mM), glutathione (GSH, 5 mM) and HEPES (10 mM, pH 7.2). To prevent the possible formation of any microscopic gas bubbles while lowering the initial oxygen partial pressure from air at one atmosphere (~154 mmHg) to something closer to the *in vivo* situation, the CELL solution was stirred under reduced pressure before being used to fill the vials. To evaluate the oxygen depletion g-value and kinetics of ROD, 30 Gy doses were delivered to these solutions at both conventional (Conv - 0.5 Gy/s) and FLASH (100 Gy/s) dose rates while pO_2 was continuously monitored. A single comparative experiment was also performed at 20 Gy/s.

To test the effects of intermediate pO_2s, 10 and 30 Gy doses were repeatedly delivered to separate vials of CELL at 0.5, 20, and 100 Gy/s until total oxygen depletion was achieved. These depletion values were grouped into 3 initial pO_2 ranges: 5–20, 20–50, and 50–100 mmHg. After complete oxygen depletion, each vial was stirred for ~20 min before the final pO_2 measurement was obtained to check the stability of the pO_2 measurement. Control experiments were performed to evaluate effects of 100–500 μM hydrogen peroxide on phosphorescence lifetime in both phosphate buffer and CELL.

Radiochemical Oxygen Depletion In Vivo

Eight to 10-week-old female C57BL/6 mice (The Jackson Laboratory) were maintained in AALAC-accredited facilities and all procedures were approved by the Institutional Animal Care and Use Committee (IACUC) at the University of Pennsylvania (Philadelphia, PA).

Fibrosarcoma syngeneic tumors were established after a subcutaneous injection over the right thigh muscle of 5×10^5 *LSL-Kras*G12D/wt; p53FL/F GEMM model cells [C57Bl/6 background (29)]. Irradiations and oxygen measurements were performed when tumors reached a volume of 200–300 mm^3.

At twenty-four hours prior to irradiation and oxygen measurements, the right thigh muscle or thigh tumor of each control or tumor-bearing mouse was injected with 20 μl of 100 μM phosphorescent probe (Oxyphor PtG4). The mice were euthanized after oxygen measurements were completed.

Mice were anesthetized for all oxygenation measurements and irradiations using 1.5% isoflurane in atmospheric gas supplied through a nose cone. Animals were placed on a heating pad to maintain body temperature at 37°C. Tissue oxygen levels were monitored for several minutes before, during and after irradiation to gather a baseline for tissue oxygenation under anesthesia. Additionally, oxygenation measurements for some mice (demarcated below) were performed using the integral laser as the source of excitation to reduce the illuminated volume to selectively measure the signal originating from probe located inside the tumor.

RESULTS

The capability of the phosphorescence quenching method to measure oxygen at both high -and low-proton dose rates was discussed in detail in a previously published article (27).

Radiochemical Oxygen Depletion in Solution

Oxygen depletion experiments were performed at 100 and 0.5 Gy/s. For successive doses of 30 Gy and then 10 Gy, the oxygen pO_2 decreased in stepwise fashion with each dose and for both dose rates (Fig. 2). On the timescale of the whole experiment (500–1,000 s) the derived values showed no observable noise [i.e., values within the thickness of the line (Fig. 2A and C)]. However, using a highly expanded timescale of the FLASH pulse, significant noise could be observed (Fig. 2B). This did not affect measurements either immediately before or after the dose administrations and was caused by radiation-field induced light pulses (27). Except for very low-oxygen partial pressures (see below) the g-values for 10 Gy doses were within 2% of the values for 30 Gy depletions, so to summarize the g-values for conventional, FLASH, and an intermediate dose rate (20 Gy/s) the data were combined and yielded the following results. The g-value above pO_2 = 20 mmHg, averaged over all doses, decreased with an increase in dose rate from 0.54 mmHg/Gy at 0.5 Gy/s, through 0.45 mmHg/Gy at 20 Gy/s, and finally 0.40 mmHg/Gy at 100 Gy/s (Fig. 3A). This decrease corresponded to a 25.9% lower g-value for FLASH relative to conventional radiation dose rates.

The g-value for ROD was plotted against the pO_2 at the time of irradiation to elucidate its pO_2 dependence at each of the three tested dose rates. The g-value remained constant (within experimental error) from 100 to 20 mmHg pO_2, then decreased by 30% (Conv), 43% (20 Gy/s), and 41% (FLASH) at ~10 mmHg, and continued to decrease until the solution was anoxic (Fig. 3B). No recovery in pO_2 was observed after 20 min of stirring

postirradiation for any of the samples suggesting that the vials were completely sealed against external oxygen leakage.

Radiochemical Oxygen Depletion in Normal Muscle and Sarcoma Tumor

The pO_2 in normal thigh muscle had a mean value of 31.1 mmHg (range: 18.3–42.8 mmHg; Table 1, average of reported values). Tissue oxygen levels fluctuated during pre- and postirradiation monitoring by up to 20 mmHg (60% of their initial value). Thus, the mice were given several minutes after anesthesia and setup to allow the pO_2 to reach a stable value before radiation was initiated. The delivery of 30 Gy at conventional dose rate did not significantly alter the normal tissue pO_2 (n = 4) (see Fig. 4A for an example result with summary in Table 1). In contrast, the same 30 Gy delivered at FLASH dose rate resulted in a sharp decrease in pO_2 with a mean decrease of 8.5 mmHg (n = 7) (see Fig. 4A and B for example results). For 60 Gy at FLASH dose rate, the mean pO_2 reduction was 13.5 mmHg (n = 3) (Table 1), indicating a somewhat reduced g-value for oxygen depletion at this higher dose. Post FLASH, tissue oxygenation returned to the pre-irradiation level with a mean time of 7.9 s for 30 Gy and 8.1 s for 60 Gy (see Fig. 4B for example result with summary in Table 1).

Two mice were subjected to a second dose of 30 Gy after the tissue pO_2 recovered to, and stabilized at, the preirradiation level after either 30 or 60 Gy irradiation. The changes in tissue pO_2 for these “follow-up” irradiations were 8.4 and 8.1 mmHg, respectively, which lay within the standard error of tissue pO_2 change for mice that were not previously exposed to radiation (data not shown).

In contrast to the mean pO_2 of ~30 mmHg in normal muscle, the mean for tumor tissue was 13.4 mmHg (range: 7.6–24.5 mmHg; Table 1, average of reported values). As in the case of normal tissue measurements, no depletion was seen in any of the tumors during application of 30 Gy at conventional dose rate (n = 3) (see Fig. 5A for example result). However, a 30 Gy FLASH dose resulted in a sharp decrease in tissue oxygenation by 3.5 mmHg on average (n = 5) (see Fig. 5A and B for example results with summary in Table 1). Tissue re-oxygenation was much slower in tumor tissue than in normal muscle, requiring an average of 26.0 s (see Fig. 5A and B for example results with summary in Table 1).

Tumor oxygen depletion was also measured using a laser to illuminate a much smaller volume of tumor tissue (diameter of light beam for the laser was 0.2 mm vs. ~5 mm for LED and optical cable). This change did not affect the nature of the results: mean tumor tissue pO_2 was initially 16.1 mmHg (range: 4.2–30.7 mmHg; Table 1). A 30 Gy FLASH dose resulted in a mean pO_2 decrease of 3.9 mmHg/Gy (n = 4) (Table 1). The time for tumor tissue reoxygenation was also consistent with that using the LED/ optical cable light source, requiring 30.3 s for recovery (Table 1).

Combining the pO_2 depletion data for normal tissue and tumors, the magnitude of oxygen depletion showed a positive correlation with the initial oxygen concentration (Fig. 6).

In a few mice, the oxygen levels in both types of irradiated tissue were measured 24 h postirradiation to determine whether any obvious changes had occurred. No changes were

observed in mice irradiated at either FLASH or conventional dose rates (data not shown). This demonstrates stability of not only the tissue pO_2, but also the injected dye.

DISCUSSION

In this study we confirmed that a commercial phosphorometer modified for rapid sampling could assess ROD during proton FLASH in normal muscle (27) and in a murine sarcoma model (GEM sarcoma). We also found that ROD g-values in solutions mimicking the radical scavenging and reducing environment of intracellular milieu (glycerol, glucose, glutathione, HEPES buffer) were higher than in solutions of proteins (such as bovine serum albumin) or simpler solutions without glutathione (25, 27).

In a recent study, using the same instrument but without the rapid sampling modification, Cao et al. found that light generated by an electron beam “blinded” the instrument during the FLASH pulse thereby preventing the measurements (25). Due to this technical limitation, they reported ROD roughly 0.5 s after the pulse in both normal and tumor tissue, as well as in solutions containing BSA. The reported g-values *in vivo* were much lower than would be anticipated from their solution results and the *in vivo* g-values values measured in the present study. The reasons for these differences are not known. However, the method of the probe delivery in the former compared with the present study was different, i.e., systemic delivery via tail vein injection versus direct injection into the extravascular space. Thus, it is possible that there was more blood-associated probe in the former study (25). Any probe associated with blood would be dramatically buffered against pO_2 change by the red cell hemoglobin, close to 9 mM for oxygen-saturated blood, and would also be associated with the vascular rather than tissue pO_2.

In agreement with the study by Cao et al. (25) using a pulsed electron beam for the radiation source, we confirmed for protons that ROD in chemical solutions was lower for FLASH than conventional dose rates. This decrease in ROD for FLASH has importance because of the recent suggestion that FLASH might cause the reverse, an increased ROD compared with conventional (15). This suggestion was argued against based on radiation chemistry data showing that chain reactions (e.g., for lipid peroxidation) were enhanced at lower, as opposed to higher, dose rates (30, 31) and our results support this argument.

One of the more interesting and novel aspects of the studies by Cao *et al.*, as well as the data reported herein, is that the magnitude of the ROD difference between conventional and FLASH for chemical solutions (e.g., for solutions of BSA or glycerol/glutathione) was similar to the protection factor by FLASH seen in normal tissue – of the order of 20–30% (3–5, 25, 27). There is no way to test whether this difference holds *in vivo* (where the FLASH effect is observed) since the ROD occurring during conventional irradiation was masked by oxygen resupply from the vasculature. This testing problem is further complicated by the lack of a FLASH radioprotective effect for tumor tissue or for cells *in vitro*. Thus it might be tempting to think of “oxidation is bad” as a general aspect of radiation response. This is clearly not the case since the presence of thiols increases ROD, yet is critical for radiation protection by the oxygen effect (32). In other words, some aspects of ROD may be associated with increased damage, while others, the reverse.

One might not expect such a lack of clarity regarding radiochemical oxidation mechanisms considering the long history of radiation chemistry studies related to the oxygen effect (31, 33). However, much of radiation chemistry has employed pulse radiolysis methods with dose rates much higher than FLASH (31) and without corresponding information at low dose rates. Additionally, most radiation chemistry studies have used predominantly single-radical systems (e.g., via radical converters such as nitrous oxide and formate) designed to elucidate reactions and their rate constants, not mixed substrates and radicals as used here. Thus, there is a paucity of literature data where ROD was measured directly (12, 13, 32). Most prior studies monitored ROD indirectly by changes in the radiation response at levels of pO_2 defined before irradiation or utilized ROD to cause hypoxia in studies of the time course of the oxygen effect (11, 34, 35). *In vivo*, ROD as a cause of radioprotection via the oxygen effect [threefold increase in radiation resistance as oxygen decreases to very low values (32)] was most completely investigated by Hendry, who observed protection of mouse tail against radionecrosis at very high dose rates (36). In Hendry's study, it was proposed that for protection to occur by ROD, the stem cells must exist at a low pO_2 (compared with normoxia; 30–70 mmHg), and the dose needed to be high enough to change the radiation response through ROD. Although this observation cannot be referred to as the first instance of the "FLASH effect", since no tumor information was included, similar considerations have recently been employed to model the effects of FLASH (14). In this and other modeling studies a major stumbling block has been a convincing explanation for why there is a lack of protection by FLASH for tumors. One proposed explanation is that since tumors exist at a substantially lower pO_2 than does normal tissue, additional ROD might cause little further radiation protection (3, 4, 14). An additional contributing factor might be the lower g-value for ROD observed in tumors compared with normal tissue [(25) and present study]. Additionally, in the most recent paper a substantial oxygen-dependence to ROD has been observed at levels below 20 mmHg (27), also observed in the present study. This would directly lead to a reduced ROD in tumor versus normal tissue, and could at least partially explain why FLASH does not protect tumor. With one exception (37) ROD has not previously been reported to be oxygen-concentration dependent (12, 13, 32). Thus, a great deal more information on the specific mechanisms of ROD is needed.

Several recent studies have tried to model the FLASH effect using radiolysis of pure water at times of up to 1 μs with all the reducing radicals (free electrons and hydrogen atoms) reacting with oxygen to produce superoxide and hydroperoxy radicals (17, 37). The impact of highly oxidizing hydroxyl radicals has been ignored or limited to removal of some of the reducing radicals. However, tissue is drastically different from pure water in terms of both the mechanisms and magnitude of ROD (31). If approximated as a homogeneous medium, tissue contains more than an ~1 M "solution" of macromolecular subunits also containing many low molecular weight solutes in high millimolar concentrations. Many of these molecules will react with primary radicals (hydrated electron, hydrogen atom, hydroxyl radical) at extremely high rates limited by the diffusion of the latter. In view of this complexity, the choice of experimental (as well as computational) models for adequate representation of the underlying chemistry may be critically important.

In two previous studies (25, 27) solutions of albumin were used to quantify the magnitude of ROD. While albumin is easily accessible and can be used to verify that ROD in

the presence of organic matter is different from that in pure water (31) it may better describe the extracellular rather than intracellular milieu. The solubility of albumin limits concentration of its aqueous solutions to ~5% (by weight; ~0.8 mM in protein but ~450 mM amino acid subunits) compared to 20% protein content of cells. Furthermore, many important components of the intracellular milieu are missing in albumin solutions (e.g., lipids, reducing agents).

One possible approach to model the intracellular environment used in the present study was based on work from the 1990s that wrestled with the unexpected radiation response of phage DNA to ionizing radiation. When phage were irradiated in simple buffers, the phage DNA was found to be not only vastly more radiosensitive than *in vivo*, but also exhibited a reverse oxygen effect, i.e., the DNA was protected in the presence of oxygen [see ref. (28) and references therein]. Several studies subsequently showed that a normal oxygen effect could be established by including thiols in experimental solutions. The radiation sensitivity discrepancy was solved by including hydroxyl radical scavengers at high concentrations (28). Obviously, the resulting “CELL” solution cannot mimic all aspects of the enormously complex intracellular environment. Nevertheless, it is a step forward and might be analyzable from a radiation chemistry perspective.

Although there are substantial differences between the present data and the recent results using electrons (25), there are some solid parallel findings. First, for model solutions ROD is substantially less (~25%) for FLASH than for conventional dose rates. Second, both studies found no measurable ROD *in vivo* for conventional dose rates, consistent with the expected rapid resupply of oxygen from the vasculature. Third, there appears to be an agreement that ROD in less oxygenated tissues (e.g., tumors) is less than in normal tissues. Finally, both studies were able to monitor post-FLASH radiation oxygen recovery, and the time scales for oxygen recovery were similar for normal tissue (a few seconds). In tumor tissue, the recovery periods were much longer in the present study but the recovery periods are likely to be tumor-model dependent.

CONCLUSIONS

Using the newly developed variant of the phosphorescence quenching method we determined that proton FLASH depletes ~25% less oxygen per Gy than conventional dose rates for a solution that partially mimicked the intracellular environment (CELL). *In vivo*, the ROD g-values were significantly higher than expected based on previously published results. Unlike conventional dose rate irradiation, FLASH caused oxygen to be depleted faster than it could be replaced from the vasculature. The magnitude of the ROD was higher in normal tissue than in tumors. Considering that the FLASH effect has been reported to occur *in vivo* at doses as low as 10 Gy, it is difficult to reconcile the amount of protection observed as being due to oxygen depletion alone. In cell-mimicking solutions the oxygen depletion g-vales were significantly higher than found *in vivo*. It is worth re-emphasizing that the phosphorescent probe used in this study was confined to the extracellular space and it is possible that intracellular oxygen depletion was greater than observed herein.

ACKNOWLEDGMENTS

Support of the grants P01 CA257904-01A1 (RDW, CJK), HL145092 (MEK), EB027397 and EB028941 (SAV) from the National Institutes of Health, and developmental funds from the Department of Radiation Oncology, University of Pennsylvania Perelman School of Medicine is gratefully acknowledged. SAV has partial ownership of Oxygen Enterprises Ltd. which owns the intellectual property for phosphorescent probes technology (US Pat. No. 9,556,213; US, 2017/0137449 A1). All other authors declare no competing interests.

REFERENCES

1. Hall EJ. In: Radiobiology for the Radiologist. J. B. Lippincott, Philadelphia; 1988.
2. Wilson JD, Hammond EM, Higgins GS, Petersson K. Ultra-high dose rate (FLASH) radiotherapy: silver bullet or fool's gold. Front Oncol. 2019; 9:1563. [PubMed: 32010633]
3. Favaudon V, Caplier L, Monceau V, Pouzoulet F, Sayarath M, Fouillade C, et al. . Ultrahigh dose-rate FLASH irradiation increases the differential response between normal and tumor tissue in mice. Sci Transl Med. 2014; 6:245ra93.
4. Montay-Gruel P, Petersson K, Jaccard M, Boivin G, Germond J-F, Petit B, et al. _Irradiation in a flash: Unique sparing of memory in mice after whole brain irradiation with dose rates above 100 Gy/s. Radiother Oncol. 2017; 124:365–369. [PubMed: 28545957]
5. Simmons DA, Lartey FM, Schuler E, Rafat M, King G, Kim A, et al. Reduced cognitive deficits after FLASH irradiation of whole mouse brain are associated with less hippocampal dendritic spine loss and neuroinflammation. Radioth Oncol. 2019;139:4–10.
6. Vozenin MC, De Fornel P, Petersson K, Favaudon V, Jaccard M, Germond J-F, et al. The advantage of FLASH radiotherapy confirmed in mini-pig and cat-cancer patients. Clin Cancer Res. 2019; 25:25–42.
7. Beyreuther E, Brand M, Hans S, Hideghety K, Karsch L, Lessman E, et al. Feasibility of proton FLASH effect tested by zebrafish embryo irradiation. Radioth Oncol. 2019; 139:46–50.
8. Diffenderfer ES, Verginadis II, Kim MM, Shoniyozov K, Velalopolou A, Goia D, et al. Design, implementation, and in vivo validation of a novel proton FLASH radiation therapy system. Int J Radiat Oncol Biol Phys. 2020; 106:440–448. [PubMed: 31928642]
9. Alper T, Howard-Flanders P. Role of oxygen in modifying the radiosensitivity of E. Coli B. Nature. 1956;178:978–979. [PubMed: 13378491]
10. Elkind MM, Swain RS, Alescio T, Sutton H, Moses WB. Oxygen, nitrogen, recovery and radiation therapy. In: Symposium on Fundamental Cancer Research. Baltimore: Williams and Wilkins; 1965; pp442–461.
11. Koch CJ, Kruuv J, Frey HE. Variation in radiation response of mammalian cells as a function of oxygen tension. Radiat Res 1973; 53:33–42. [PubMed: 4734388]
12. Koch CJ. Measurement of very low oxygen tension in liquids: Does the extrapolation number for mammalian survival curves decrease after x-irradiation under hypoxic conditions? In: Proc 6th LH Gray Conf. London: Institute of Physics. 1975; pp. 167–173.
13. Whillans DW, Rauth AM. An experimental and analytical study of oxygen depletion in stirred cell suspensions. Radiat Res. 1980; 84:97–114. [PubMed: 7005927]
14. Pratx G, Kapp DS. A computational model of radiolytic oxygen depletion during FLASH irradiation and its effect on the oxygen enhancement ratio. Phys Med Biol. 2019; 64;185005. [PubMed: 31365907]
15. Spitz DR, Buettner GR, Petronek MS, St-Aubin JJ, Flynn RT, Waldron TJ et al. . An integrated physico-chemical approach for explaining the differential impact of FLASH versus conventional dose rate irradiation on cancer and normal tissue responses. Radiother Oncol. 2019. 10.1016/j.radonc.2019.03.028.
16. Adrian G, Konradsson E, Lempart M, Back S, Ceberg C, Petersson K. The FLASH effect depends on oxygen concentration. Br J Radiol. 2020; 93:20190702. [PubMed: 31825653]
17. Alanazi A, Meesungnoen J, Jay-Gerin J-P. A computer modeling study of water radiolysis at high dose rates. Relevance to FLASH radiotherapy. Radiat Res. 2021; 195:149–162. [PubMed: 33300999]

18. Clark LC. Electrochemical Device for Chemical Analysis. United States Patent. 1959; US2913386.
19. Koch CJ. Measurement of Absolute Oxygen Levels in Cells and Tissues using Oxygen Sensors and the 2-nitroimidazole EF5. In: Meth. Enzymol Sen CK, Packer L, eds. San Diego: Academic Press; 2002; 353:3–31.
20. Hockel M, Knoop C, Schlenger K, Vordran B, Baussmann E, Mitze M, et al. Intratumor pO_2 predicts survival in advanced cancer of the uterine cervix. Radioth Oncol. 1993; 26:45–50.
21. Vanderkooi JM, Maniara G, Green TJ, Wilson DF. An optical method for measurement of dioxygen concentration based on quenching of phosphorescence. J Biol Chem. 1987; 262:5476–5482. [PubMed: 3571219]
22. Vinogradov SA, Lo L-W, Wilson DF. Dendritic polyglutamic porphyrins:probing porphyrin protection by oxygen-dependent quenching of phosphorescence. Chem Eur J. 1999; 5:1338–1347.
23. Lebedev AY, Cheprakov AV, Sakadzic S, Boas DA, Wilson DF. Vinogradov SA. Dendritic phosphorescent probes for oxygen imaging in biological systems. ACS Appl. Mater Interfaces 2009; 1:1292–1304. [PubMed: 20072726]
24. Esipova TV, Karagodov A, Miller J, Wilson DF, Busch TM, Vinogradov SA. Two new “protected” Oxyphors for biological oximetry: properties and application in tumor imaging. Anal Chem. 2011; 83:8756–8765. [PubMed: 21961699]
25. Cao X, Zhang R, Esipova TV, Allu SR, Ashraf R, Rahman M, et al. Quantification of oxygen depletion during FLASH irradiatiion in vitro and in vivo. Int J Radiat Oncol Biol Phys. 2021; 111:240–248. [PubMed: 33845146]
26. Helo Y, Kacperek A, Rosenberg I, Royle G, Gibson AP. The physics of Cerenkov light production during proton therapy. Phys Med Biol. 2014: 59: 7107–7123. [PubMed: 25365447]
27. El Khatib M, Van Slyke AL, Velalopoulou A, Kim MM, Shoniyozov K, Allu SR, et al. Ultrafast tracking of oxygen dynamics during proton FLASH. Int J Radiat Oncol Biol Phys. 2022: online ahead of print. DOI: 10.1016/j.ijrobp.2022.03.016
28. Ayene IS, Koch CJ, Krisch RE. Simulation of the cellular oxygen effect with an SV40 DNA model system using DNA strand breaks as an endpoint. Radiat Res. 1996: 146:501–9. [PubMed: 8896576]
29. Castle KD, Kirsch DG. Establishing the impact of vascular damage on tumor response to high-dose radiation therapy. Cancer Res. 2019; 79:5685–5692. [PubMed: 31427377]
30. Koch CJ. Re: Differential impact of FLASH versus conventional dose rate irradiation: Spitz et al. Radioth Oncol. 2019; 139:62–63.
31. Wardman P. Radiotherapy using high-intensity pulsed radiation beams (FLASH): a radiation-chemical perspective. Radiat Res 2021; 194:607–617.
32. Koch CJ. The mechanism of radioprotection by non-protein sulfhydryls: Cysteine, Glutathione and Cysteamine. In: Radioprotectors: Chemical, Biological and Clinical Perspective; Bump EA, Malaker K, eds. CRC Press, Boca Raton FL 1998; pp25–52.
33. Wardman P. Time as a variable in radiation biology: the oxygen effect. Radiat Res. 2016; 185:1–3. [PubMed: 26731298]
34. Epp ER, Weiss H, Ling CC. Irradiation of cells by single and double pulses of high intensity radiation: oxygen sensitization and diffusion kinetics. Curr Top Radiat Res Q. 1976; 11:201–250. [PubMed: 826371]
35. Adams GE, Michael BD, Asquith JC, Shenoy MA, Watts ME, Whillans DW. Rapid-mixing Studies on the Time-scale of Radiation Damage in Cells. In: Nygaard OF, eds. Radiation Research: Biomedical, Chemical and Physical Perspectives. New York: Academic Press; 1975; pp478–492.
36. Hendry JH, Moore JV, Hoddgson BW, et al. The constant low oxygen concentration in all the target cells for mouse tail radionecrosis. Radiat Res. 1982; 92:172–181. [PubMed: 7134382]
37. Jansen J, Knoll J, Bayreuther E, Pawelke J, Skuzza R, Hanley R, et al. Does FLASH deplete oxygen? Experimental evaluation for photons, protons, and carbon ions. Med Phys. 2021; 48:3982–3990. [PubMed: 33948958]

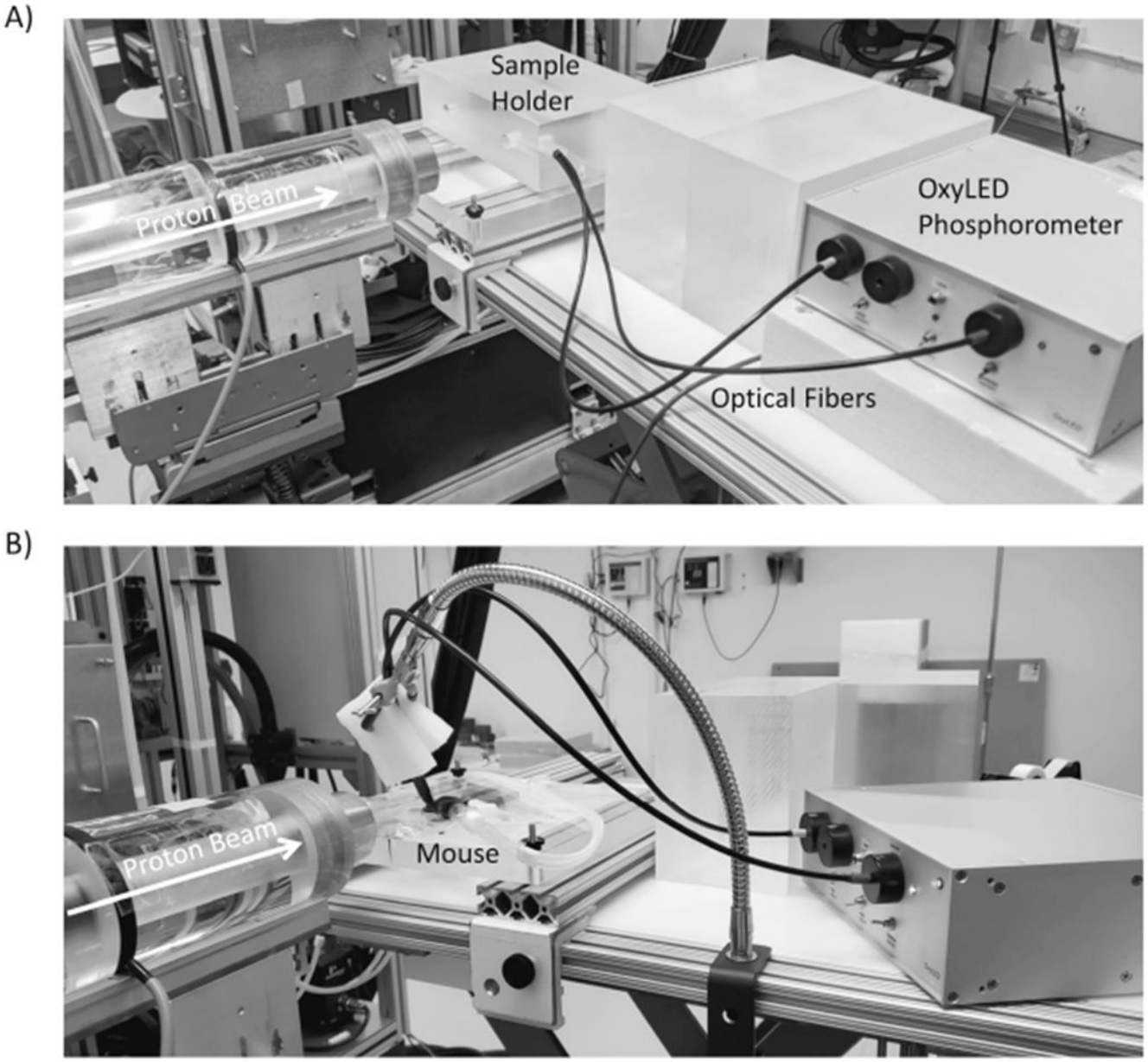

FIG. 1.

Panel A: Proton irradiation setup. A photo of the measurement setup used for ultrafast measurement of oxygen partial pressure in solutions during proton irradiation. Protons enter from the left side of the image through the beam collimator. The phosphorometer used to monitor oxygen partial pressure in either glass vials or in mice, is shown on the right. The sample holder for the vials was an acrylic block designed to hold the glass vial in the beam and position the optical fibers orthogonal to the beam axis to provide excitation and collect emission from the PtG4 phosphorescent probe in solution. Panel B: For *in vivo* experiments, the sample holder block was replaced by a heating pad to which the mice were taped while breathing anesthetic gas.

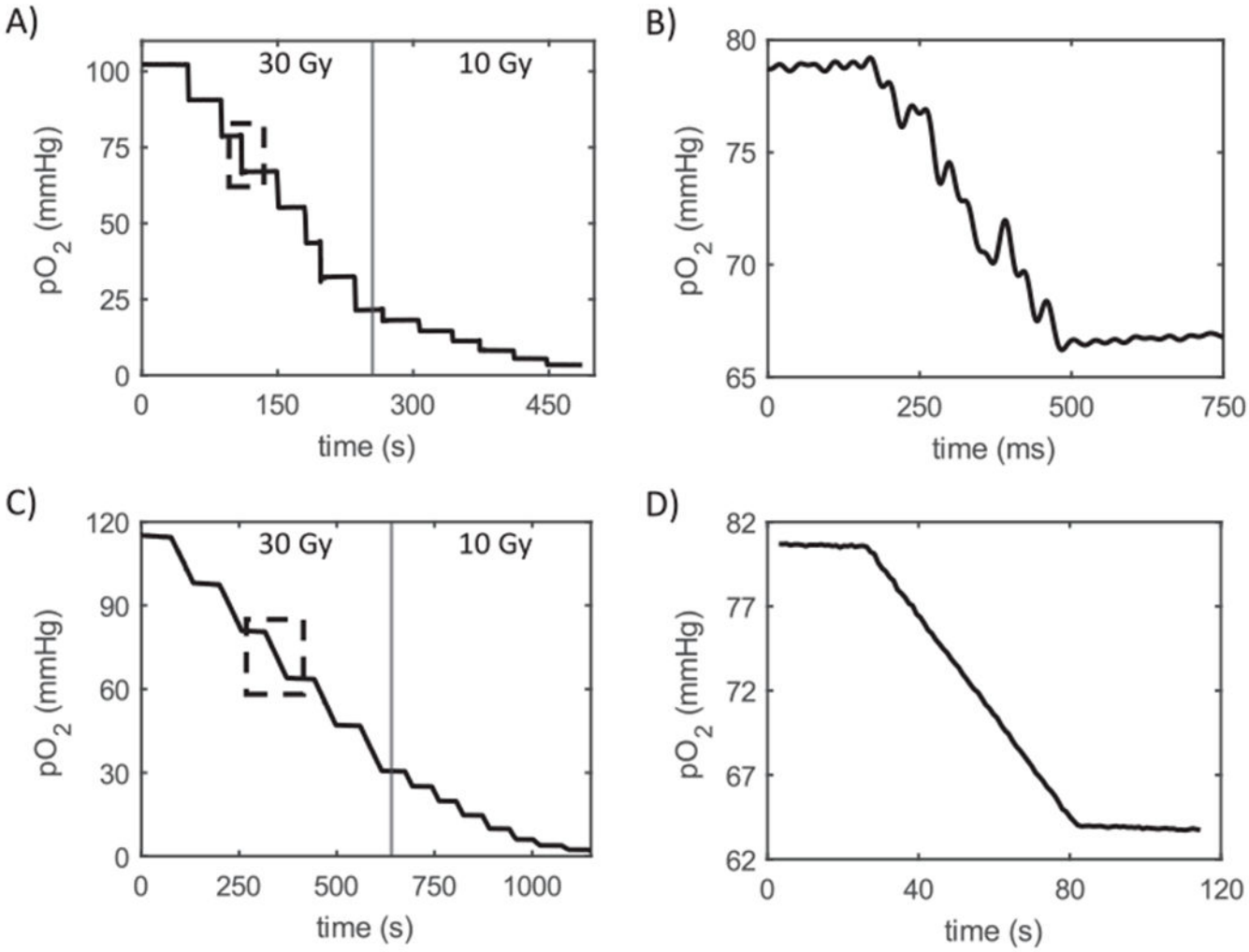

FIG. 2.

Oxygen depletion in solution described as “CELL” in Methods section. Panel A: Oxygen partial pressure monitoring during seven FLASH deliveries of 30 Gy followed by six deliveries of 10 Gy to the cell mimetic solution. Stepped line indicates continuous monitoring with data points averaged over several hundred decay times. Vertical line inside rectangle indicates data taken at 3 kHz without averaging (expanded in panel B). Central vertical line divides 30 Gy (left) and 10 Gy (right) dose deliveries. Panel B: Magnified region displaying oxygen partial pressure during delivery of 30 Gy at 100 Gy/s. Note that the observed noise is averaged out for the longer timescale depicted in panel A. Panels C and D: Recapitulation of panels A and B but for conventional dose rate. Due to the higher ROD g-value for conventional compared with FLASH, only 5 deliveries of 30 Gy were made. In this and subsequent figures the X-axis “Time (s)” indicates time from the start of each individual data file.

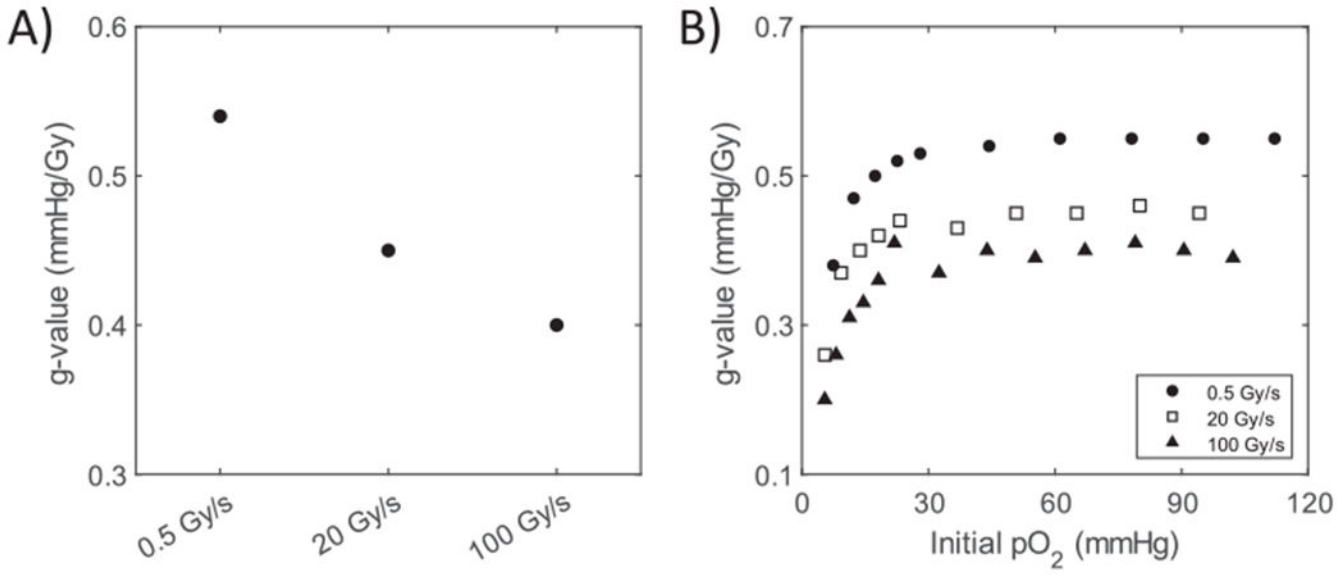

FIG. 3.

Dose rate and oxygen partial pressure effects in solutions of "CELL". Panel A: Plot of the dose rate dependence of the ROD g-value for a 30 Gy exposure at 3 dose rates displaying a slow decrease from 0.5 Gy/s to 100 Gy/s. Panel B: Effect of initial pO_2 demonstrating the decrease in ROD g-value below about 20 mmHg.

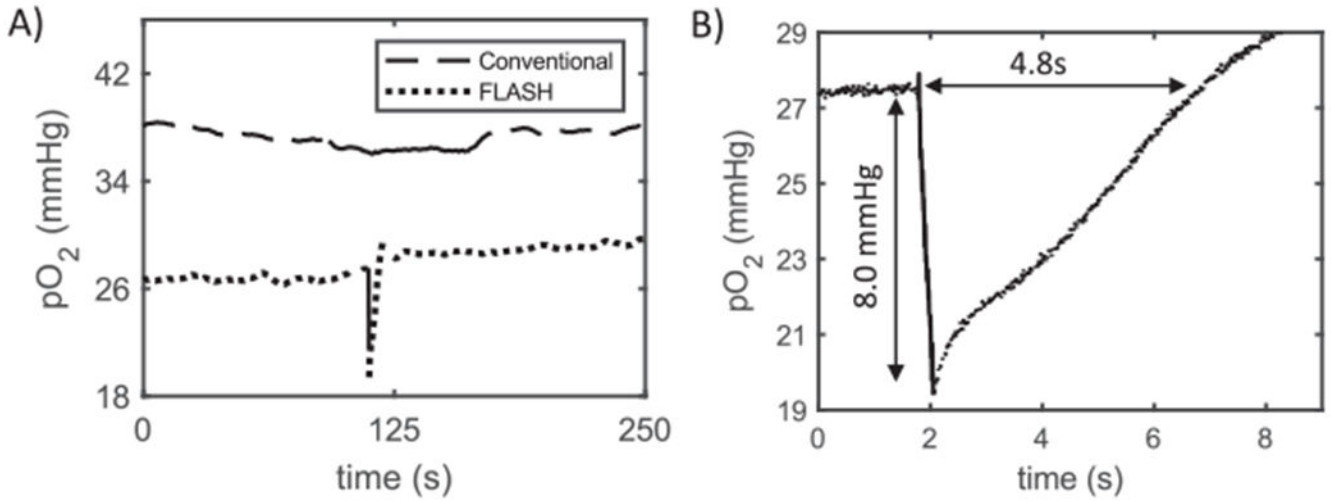

FIG. 4.

Examples of ROD in normal murine muscle tissue. Panel A: Plot of partial pressure of oxygen in the thigh muscle during the delivery of a 30 Gy dose at both conventional (upper curve, dashes) and FLASH (lower curve, dots) dose rates. The time during which radiation was delivered is shown by the solid portion of each curve, roughly at the central portion of total time. Panel B: Magnified temporal view (measurements recoded at 3 kHz) of the ROD due to FLASH irradiation and the subsequent recovery, for the pulse shown in panel A. Depletion value and recovery time for this example are displayed on graph.

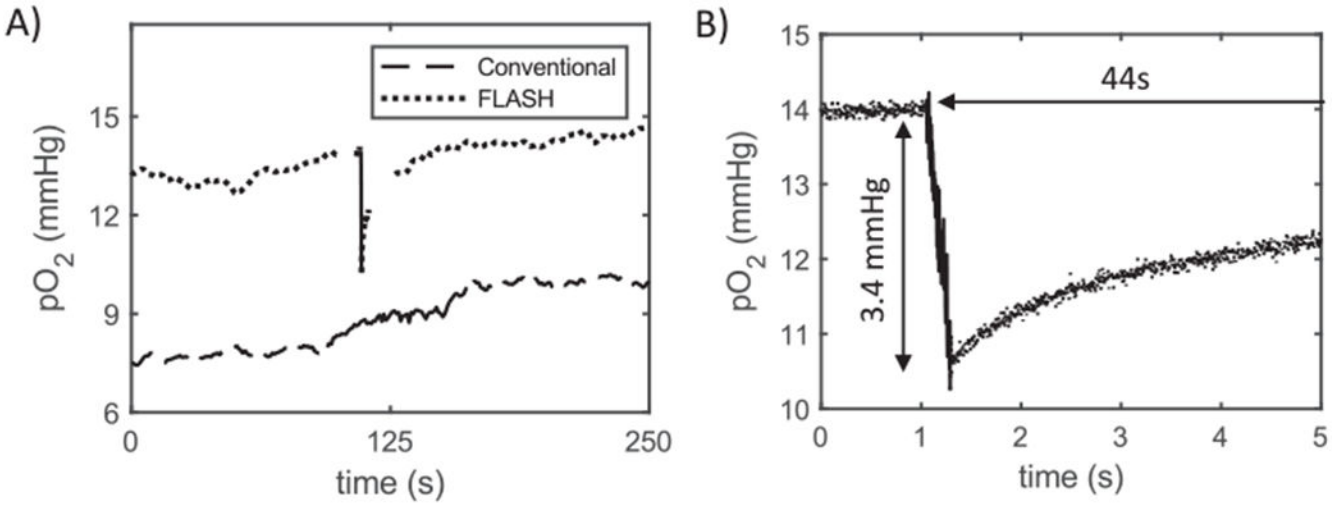

FIG. 5.

Examples of ROD in murine sarcoma tumor tissue. Panel A: Plot of partial pressure of oxygen in sarcoma tumor during the delivery of a 30 Gy dose at both conventional (lower curve, dashes) and FLASH (upper curve, dots) dose rates. The period during which radiation was delivered is shown by the solid portion of each curve, roughly at the central portion of total time. Panel B: Magnified temporal view (measurements recoded at 3 kHz) of the ROD due to FLASH irradiation and the subsequent recovery, for the pulse shown in panel A. Depletion values and recovery times displayed on graph. Note that recovery time extends well beyond the length of the ultrafast measurement window (5 s).

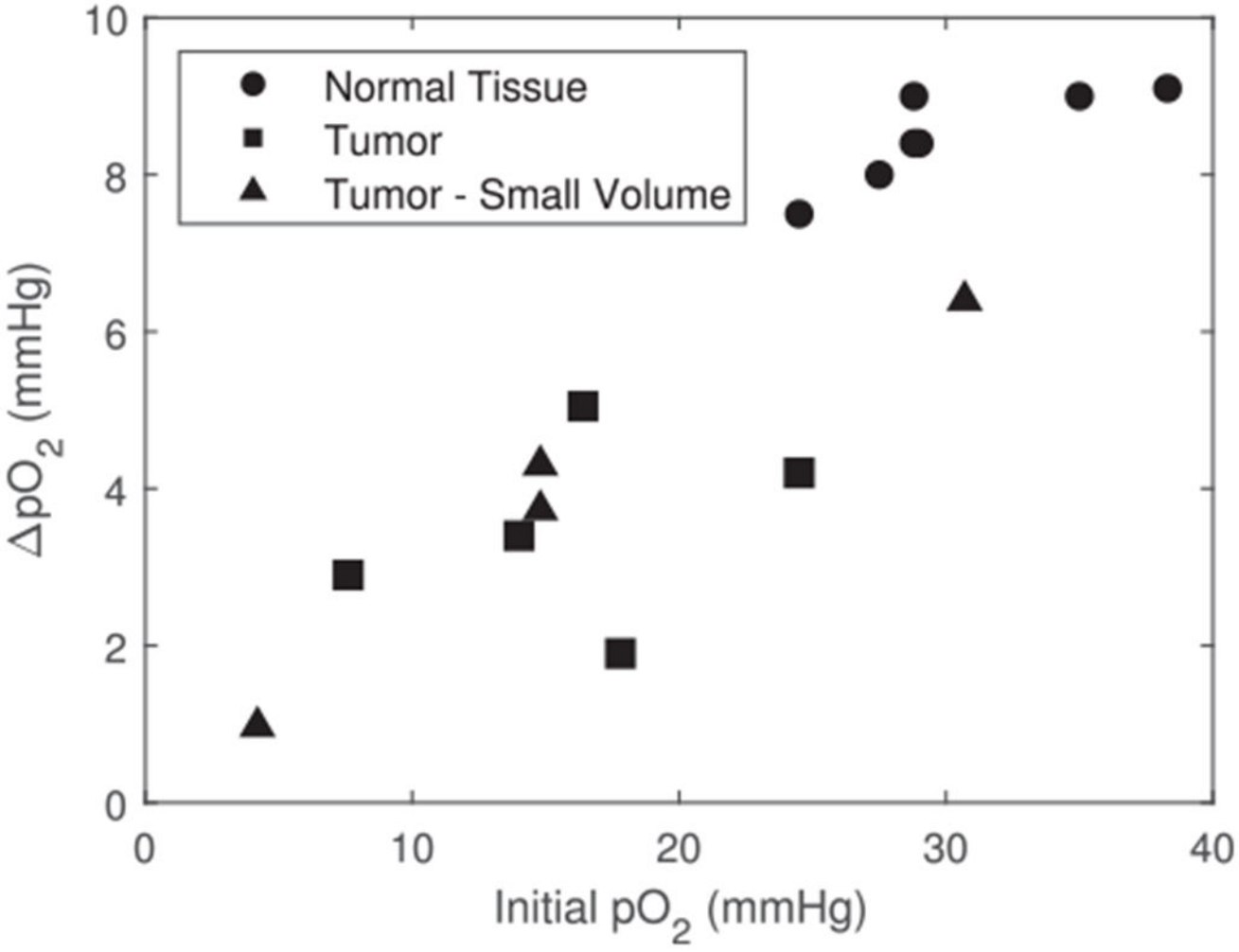

FIG. 6.

Dependence of ROD on the initial tissue pO_2 for 30 Gy at FLASH dose rates (combined normal and tumor tissue). The change in pO_2 shows an overall positive correlation for all FLASH data including normal tissue (closed circles, LED light source) and tumor tissue (closed squares, LED light source; closed triangles, - laser light source).

TABLE 1

In Vivo Oxygen Depletion Results Summary

Dose rate	Tissue type	Initial pO_2 (mmHg)	pO_2 depleted (mmHg)	G value (mmHg)	Recovery time (s)	Recovery rate (mmHg)	Number of mice
FLASH							
	Normal						
	Male	32.78 ± 2.34	8.71 ± 0.18	0.29 ± 0.01	9.90 ± 0.51	0.89 ± 0.05	n = 4
	Female	26.94 ± 1.27	8.19 ± 0.43	0.27 ± 0.01	5.15 ± 0.30	1.59 ± 0.04	n = 3
	Combined	30.27 ± 1.79	8.50 ± 0.22	0.28 ± 0.01	7.86 ± 1.00	1.19 ± 0.15	n = 7
	Tumor						
	Male	16.06 ± 2.74	3.49 ± 0.54	0.12 ± 0.02	26.00 ± 4.93	0.15 ± 0.03	n = 5
	Male laser diode	16.13 ± 5.46	3.85 ± 1.12	0.13 ± 0.04	30.25 ± 5.11	0.13 ± 0.03	n = 4
Conventional							
	Normal muscle						
	Male	37.7	−0.83 *	−0.03 *	NA	NA	n = 1
	Female	32.92 ± 2.64	0.88 ± 0.19	0.03 ± 0.01	NA	NA	n = 3
	Combined	34.11 ± 2.21	0.46 ± 0.44	0.02 ± 0.01	NA	NA	n = 4
	Tumor						
	Male	8.87 ± 1.06	−0.78 ± 0.07 *	−0.03 ± 0.00 *	NA	NA	n = 3
FLASH 60 Gy							
	Normal muscle						
	Male	8.87 ± 7.27	13.50 ± 1.67	0.22 ± 0.03	8.10 ± 0.62	1.71 ± 0.31	n = 3

Note. Gender specific and aggregate data sets for normal and tumor tissue irradiated at both FLASH and Conv dose rates. Data shown is mean ± SEM.

* Negative values denote an increase in pO_2 during irradiation.